2014 IEEE International Conference on Robotics & Automation (ICRA)
Hong Kong Convention and Exhibition Center
May 31 - June 7, 2014. Hong Kong, China

Rapid Acceleration and Braking: Inspirations from the Cheetah's Tail

Amir Patel*, *Student Member, IEEE* and M. Braae*, *Member, IEEE*

***Abstract*— Stimulated by recent biomechanics research of the cheetah, a novel tail controller system for rapid acceleration and braking is presented. To understand the targeted behaviour of a cheetah performing a longitudinal manoeuvre and the effects an actuated tail has, a simple mathematical template was developed. Subsequently feedback controllers were designed based on our hypothesis. Finally, the control system was experimentally tested on a reduced order robot model which increased its manoeuvrability considerably.**

I. Introduction

A recent biomechanics study [1] indicates that the cheetah (*Acinonyx jubatus*) is not only the fastest terrestrial animal but possibly also the most manoeuvrable. In their findings, the authors suggest that the animal's ability to rapidly brake and accelerate could be assisted by the animal's lengthy tail. However, if the cheetah is using its tail for these manoeuvres, what is the neuromechanical strategy for doing so?

The biomechanics literature defines *Manoeuvrability* as an animal's ability to change its velocity vector in a controlled manner [2] [3]. This consists of either the ability to change the body's velocity magnitude (braking/accelerating) or adjusting its direction (turning). The dexterity with which an animal can do so is crucial for its survival. Nevertheless, our understanding of these transient and dynamic manoeuvres is still very limited as stated by Alexander [4].

This investigation was inspired by the "*Pitch then Power Model"* by Williams et al. [5]. In their study the authors demonstrate that a quadruped animal's ability to accelerate and brake is limited by its avoidance of toppling over (much like a motorcycle "popping a wheelie"). Toppling arises due to the force (propulsive or braking), causing a net moment about the COM. We hypothesise here that the cheetah can employ the tail as an actuator in a pitch rate control loop to negate this effect. This would allow it to circumvent the aforementioned model.

Furthermore, our hypothesis is motivated by various wildlife videos of the cheetah in pursuit of prey where it can be seen actuating its tail while manoeuvring. Additionally, this particular study is enthused by video observations (see Fig. 1.) of cheetahs at the Cheetah Outreach conservation centre in Cape Town, South Africa.

Corresponding author: a.patel@uct.ac.za. *Department of Electrical Engineering, University of Cape Town, South Africa

Fig. 1. A cheetah is shown rapidly braking while chasing a lure during a weekly exercise run. Note the motion of the tail in the sagittal plane. (Filmed by one of the authors at Cheetah Outreach in Cape Town, South Africa).

Animals employ tails for a broad range of tasks including airborne attitude control [6] and disturbance rejection [7]. Inspired by this, various researchers have successfully implemented attitude control and disturbance rejection on robotic platforms [8] [9] [10] [11]. Moreover, tails have been proven to be more effective at short timescale manoeuvres than reaction wheels [8] [11].

Specific applications of robotic tails for manoeuvrability tasks have also been implemented. Kohut et al. have successfully implemented rapid turning on a hexapod using an actuated tail [12] [13]. Also, drawing inspiration from the cheetah's tail, Patel & Braae have successfully implemented tail control systems for rapid turning at high-speed [14] and rapid acceleration on a simulated quadruped [15].

This paper will investigate the use of an actuated tail for rapid acceleration and braking manoeuvres. Firstly, in Section II following the paradigm of biomechanical templates [16], we develop a reduced-order dynamic model to describe the targeted behaviour of an animal (a cheetah in our case) performing an acceleration (or braking) manoeuvre. Here, simple models with and without a tail are compared and it is shown that with a tail actuator, more aggressive acceleration manoeuvres are possible. In Section III and IV, we will refine the model for the robotic test platform that was developed. This section also includes the design of novel tail controller algorithms as well as simulation of rapid acceleration and braking manoeuvres. In Section V, the experimental results are provided for the robotic platform. Finally, Section VI discusses the experimental results from which conclusions are drawn and future avenues of research are recommended.

978-1-4799-3684-7/14/$31.00 ©2014 IEEE

II. The Longitudinal Manoeuvre Template

Templates and anchors are a concept utilized to explain control strategies for animal locomotion [16]. Animals elegantly employ a synergy of muscles to perform high-level (task) behaviour. In essence, animals are often considered to be hyper-redundant but their task-level behaviour can be described by reduced-order models called *Templates* [17]. Well known templates are the Spring Loaded Inverted Pendulum (SLIP) and the Lateral Leg Spring (LLS) models [18]. *Anchors* in contrast are more detailed and complex models, which closer align to the animal's morphology. Although simplistic, templates offer a powerful mechanism to provide insight into neuromechanical control.

A. Equations of Motion

Inspired by the *Pitch then Power Model* [5], we propose a template to capture the task-level behaviour of a cheetah during a rapid acceleration[1] manoeuvre. This model although conservative and simple, provides valuable insight into the limitations of manoeuvrability as well as the dynamic effect a tail would have in these scenarios.

It is stated that during a rapid acceleration or braking manoeuvre, the hind and forelegs respectively are the primary forces acting on the body [5] [19]. Where, by contact with the substrate and by use of hip torque (or shoulder torque in the case for braking) the animal is propelled. If we further consider the abdomen, legs and head as one collective rigid body the mathematical model can be reduced significantly.

With the addition of an actuated tail, the proposed *Longitudinal Manoeuvre Template (LMT)* is depicted in Fig. 2.

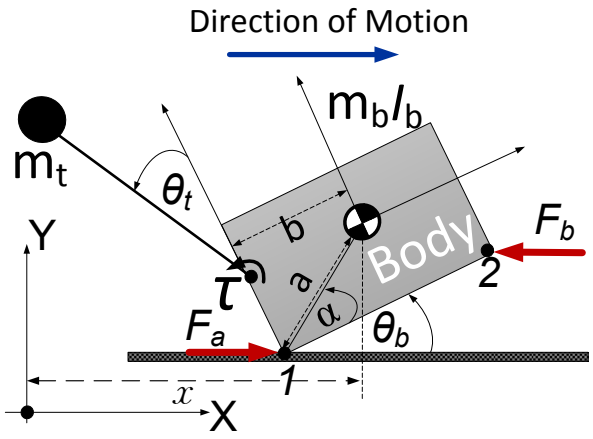

Fig. 2. The Longitudinal Manoeuvre Template (LMT) model is depicted. The model consists of a collective rigid body and a point mass tail. The model experiences either force F_a when undergoing an accelerating manoeuvre or F_b when braking.

The propulsive force (F_a) can be envisioned as a force input acting at the rear contact point of the collective rigid body with the ground. Similarly, for deceleration the force (F_b) input can be considered to be acting at the front contact point. These forces will be generated by some combination of leg actuation.

The tail is modelled as a point mass attached to an idealized massless rod of length L_t. Furthermore, the tail is actuated by an ideal torque actuator which is located some distance, b, away from the centre of mass (COM) of the collective body.

A number of assumptions were made in deriving the mathematical model. Firstly, it is assumed that during acceleration or braking only one force acts on the body. This is biomechanically accurate as for example during acceleration initiation, propulsion occurs primarily from the hind leg. Secondly, we have considered a fixed geometry. Clearly a cheetah is capable of flexing its spine which will shift the collective COM around. However, we believe that our assumptions result in a conservative model which will still provide an understanding of the limitations in manoeuvrability and the positive effects a tail can provide.

Unlike the *Pitch then Power Model*, we present a dynamic model. The system dynamics are modelled using the Euler-Lagrange method [20] [21] described by the equation[2]:

$$\boldsymbol{M}(\boldsymbol{q})\ddot{\boldsymbol{q}} + \boldsymbol{C}(\boldsymbol{q},\dot{\boldsymbol{q}})\dot{\boldsymbol{q}} + \boldsymbol{G}(\boldsymbol{q}) = \boldsymbol{B}\boldsymbol{\tau} + \boldsymbol{A}\boldsymbol{\lambda} \quad (1)$$

and the generalized coordinate vector is given by:

$$\boldsymbol{q} = [x \quad \theta_b \quad \theta_t]^T. \quad (2)$$

where, x is the COM longitudinal position of the rigid body with respect to the inertial frame, θ_b is its pitch angle with respect to the horizon and θ_t is the relative angle between the tail and body. Additionally, α, a and b are geometric properties of the collective body.

The acceleration and braking forces can be seen as generalized forces acting the body [20] and can be derived as:

$$\boldsymbol{B} = \begin{bmatrix} 1 & 0 \\ \sigma_i & 0 \\ 0 & 1 \end{bmatrix}, \quad (3)$$

with σ_i equating to $a\sin(\alpha + \theta_b)$ when accelerating and $a\sin(\alpha - \theta_b)$ when braking.

Also, note that the system contains hybrid dynamics and when the pitch angle θ_b falls to zero the constraint force (the $\boldsymbol{A}\boldsymbol{\lambda}$ term), is activated[3]. This constrains the angle and prevents the model from falling through the ground.

Now that the system dynamics have been defined, the two manoeuvres can be simulated to determine the effectiveness of the tail actuator.

B. Simulation

In order to examine the benefits of an actuated tail for manoeuvrability tasks, we simulate models with and without the tail experiencing various force magnitudes (for braking and accelerating). It is predicted from the *Pitch then Power model* that there will be a point when the respective forces will be too excessive and will result in the body toppling over.

[1] The template for the acceleration and braking manoeuvres are essentially the same except that the external force is applied at different points on the body.

[2] For the sake of brevity, the elements of the ***M, C, A*** and ***G*** matrices have been omitted as their derivation is fairly trivial.

[3] For the braking model, the pitch angle is constrained to be negative.

For the cheetah the parameters of the model are derived from geometric measurements provided by [1] [22] with the centre of mass assumed to be midpoint of the back length. The cheetah tail length is provided by [23], however to our knowledge no measurements exist for the tail mass. Thus, we will assume it is 10% of the total body mass. The parameters are summarised in Table I.

TABLE I. ESTIMATED CHEETAH MODEL PARAMETERS

Parameter	Value
Body Mass ($\boldsymbol{m_b}$)	45 (kg)
Body Roll Inertia ($\boldsymbol{I_B}$)	7.344 (kgm^2)
Tail Mass ($\boldsymbol{m_t}$)	4.5 (kg)
Tail Length ($\boldsymbol{L_t}$)	0.75 (m)
Distance to COM (**a**)	0.7 (m)
Angle to COM ($\boldsymbol{\alpha}$)	1.03 (rad)
Tail distance to COM (**b**)	0.36 (m)

As indicated previously, we hypothesise that the tail is being employed as an actuator in a pitch rate control loop. So, as a first attempt at a controller, the tail will be driven with a simple proportional controller (with a gain of 50).

The mathematical models were implemented in Simulink and numerically simulated. Each of the models (tailed and tailless) was subjected to various constant propulsive and braking forces. The simulations terminated when the body flipped over, or the tail reached its full swing of 90 degrees. The resulting pitch angles as a function of acceleration force is depicted in Fig. 3.

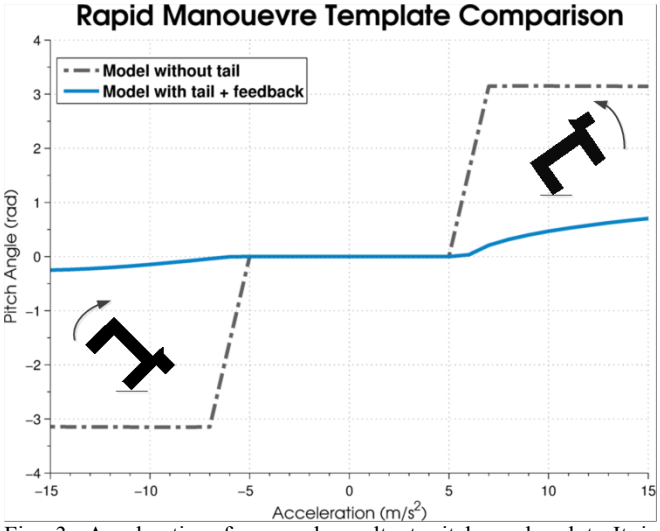

Fig. 3. Acceleration force and resultant pitch angle plot. It is evident that the tailless model topples over when accelerating aggressively. Comparatively, the model with the tail can experience greater accelerations as the resultant pitch angle is decreased.

The results for this simple simulation study are instructive. They illustrate that it is indeed possible for the cheetah to benefit from actuating its tail to negate the pitch rate incurred by manoeuvring. However, the results also demonstrate that a simple proportional controller is inadequate as a steady state error is incurred for larger magnitudes of acceleration.

With these preliminary results, the next step was to experimentally validate the hypothesis on an experimental platform.

III. ROBOT TEST PLATFORM

The *Dima* robot [14] was selected as the platform to test the rapid acceleration and braking hypothesis discussed previously. The robot is a high-speed platform previously designed to test a novel tail control system for turning at high-speed and its electrical, software and mechanical design is described in [14].

Fig. 4. *Dima* [14] was modified with a set of bevel gears to allow the tail to move in the pitch axis.

The robot's tail was modified for these tests to allow motions in the pitch axis. This was achieved by the addition of a set of bevel gears coupled to the Maxon DC motor of the tail as illustrated in Fig. 4.

One may argue the relevance of testing the hypothesis on a wheeled platform but considering the discussion in Section II, the LMT model provides a common "task encoder" [16]. For example, one can substitute the forces generated by a leg propelling the collected rigid body forwards for a wheel in contact with the ground. This is essentially the mechanism of moving from a template to an anchor. The task-level behaviour is fundamentally the same: a force is acting on a rigid body (cheetah or robot) to accelerate it.

Now that the platform has clearly been defined we delve deeper into the controller design for the two manoeuvrability tasks. These will then be simulated in order to validate them before field testing.

IV. RAPID DECELERATION

A. Force Model Identification

To implement the braking force on the body various options were considered. A pneumatic disc brake system was considered, but due to weight and space constraints this was not feasible. Ultimately, it was decided to implement an arrestor system based on a fishing reel (*Okuma Convector*) and 1mm nylon line. The line was tied in between the two front wheels and the fishing reel bolted to the ground. The reel was engaged to simulate a large deceleration force.

To adequately design the tail controllers, an accurate model of this braking force was required. We can assume that

the line behaves visco-elastically and can be modelled as a second order system [24]. Thus the force is described as:

$$F_b = E\varepsilon + \eta\dot{\varepsilon} \quad (4)$$

where, E is the elastic modulus, ε is the strain and η is the viscosity of the material. In order to estimate these parameters for this linear model, data was logged on board the *Dima* robot and rapid braking tests were performed without the tail.

The parameters were then estimated using Matlab's 'lsqnonlin' function for nonlinear curve fitting. This was done by matching the linear models coefficients to the nonlinear braking model simulation for *Dima*. The LMT model parameters for *Dima* are provided in Table II. The parameter fit and experimental data are also graphically compared in Fig. 5.

TABLE II. *DIMA* MODEL PARAMETERS

Parameter	Acceleration	Braking
Body Mass ($\boldsymbol{m_b}$)	5 (kg)	
Body Roll Inertia ($\boldsymbol{I_B}$)	0.122	0.179 (kgm^2)
Tail Mass ($\boldsymbol{m_t}$)	0.4 (kg)	
Tail Length ($\boldsymbol{L_t}$)	0.5 (m)	
Distance to COM (**a**)	0.242	0.266 (m)
Angle to COM ($\boldsymbol{\alpha}$)	1.144	0.972 (rad)
Tail distance to COM (**b**)	0.1 (m)	

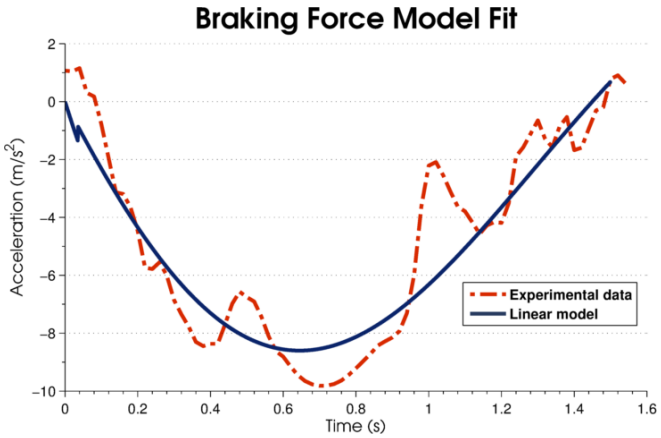

Fig. 5. Second order force model fit for the braking force induced by the nylon line is shown with E = 24.7 and η = 2.82. The simulation model was initialised at a velocity of 4.5 m/s to match the experiment conditions.

Now that the model has been satisfactorily defined, we are capable of designing the feedback control algorithms for the tail.

B. Tail Controller Design

As shown in Section II, when the LMT model experiences aggressive accelerations, it topples over. Hence, the motivation here is that if we employ the tail as an actuator for a pitch rate controller, we can counter this induced (disturbance) torque, and accelerate more aggressively.

The Longitudinal Manoeuvre Model (LMT) is nonlinear and under actuated [25]. Based on previous work done by the authors for high-speed turning, we propose the following controller architecture illustrated in Fig. 6.

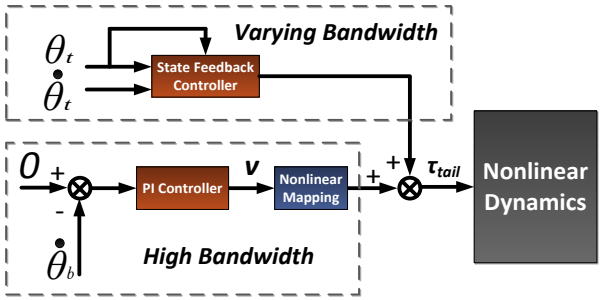

Fig. 6. Tail controller architecture implemented.

The primary goal for the controller architecture is to regulate the pitch rate of the body. As illustrated in the initial simulations of Section II a steady state error occurred. Thus, a high-bandwidth PI (proportional + integral) controller was implemented to drive the pitch rate to zero and also to diminish any modelling inaccuracy. The gains selected are k_I = 25 and k_P= 8.

Now, to map the controller's output as a torque command to the tail, a Partial Feedback Linearization (PFL) [26] was considered. However, we augment the framework presented by the authors with the addition of a disturbance term, $\boldsymbol{D}$, which is:

$$\boldsymbol{D} = \begin{bmatrix} 1 \\ \sigma_i \\ 0 \end{bmatrix} F_i, \quad (5)$$

where F_i is either the acceleration force or the braking force acting on the contact point of the collective rigid body. This will encapsulate the disturbance force that the body experiences due to acceleration/braking.

Furthermore this implies that if the actuated joint (θ_t) is commanded such that:

$$\ddot{\theta}_t = \bar{\boldsymbol{J}}^{+}[v + \boldsymbol{J_1 M_{11}^{-1}}(\boldsymbol{h_1} + \boldsymbol{\varphi_1} - \boldsymbol{D}), \quad (6)$$

where, the matrices $\bar{\boldsymbol{J}}^{+}$, $\boldsymbol{J_1 M_{11}^{-1}}$, $\boldsymbol{h_1}$ and $\boldsymbol{\varphi_1}$ are defined in [26], we then have:

$$\ddot{\theta}_b = v, \quad (7)$$

which is now a linear system.

As observed in previous studies [14], when the tail reaches its angular limits, it has significant velocity, which can negate the stabilization that it just performed when it strikes the end stops. This constraint is especially important in this study as the robot only has 90° of actuation.

In a similar manner to [14], we employ another controller, to decrease the velocity of the tail when reaching the end stops. Whereas the previous study employed a fixed gain controller relying on timescale separation, we varied the bandwidth of this "tail spring damper" as a function of the tail angle. Thus, the natural frequency scale factor of this tail damper was governed by:

$$w_{fac} = \gamma e^{(-\delta\theta_t)} \quad (8)$$

where γ are δ are parameters to be chosen. The scale factor was then multiplied by the pitch rate controller's bandwidth (5 rad/s). By pole placement, we can then set appropriate tail angle and velocity gains.

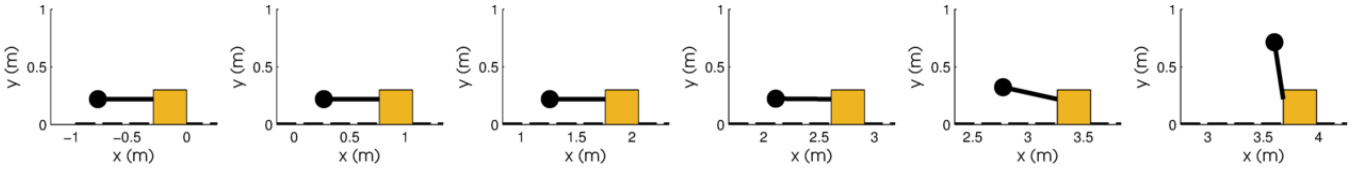

Fig. 7: Simulation of the tailed robot performing a rapid deceleration at an initial velocity of 8 m/s.

To select γ and δ for the system, numerical optimization is employed to minimize the cost function:

$$J = \int_0^{t_f} 100\dot{\theta}_b^2(t)\,dt + 0.5\dot{\theta}_t(t_f) \qquad (9)$$

Note that t_f is the simulation end time and that the weights were selected such that pitch rate damping was deemed more critical than end tail velocity. Matlab's constrained optimization 'fmincon' was subsequently utilized to determine the optimal parameters for γ and δ by simulating the full control architecture at the maximum velocity of the car (~9 m/s).

There was an evident compromise between the tail's velocity at the end of its travel and its ability to stabilize the pitch rate. After several iterations of initial solution seeds, the values of $\gamma = 2.56$ and $\delta = 9.35$ were chosen. This reduced the final tail velocity from 10 to 5 rad/s, while still providing sufficient pitch stabilization.

C. Numerical validation

The controllers were then simulated at various initial velocities to determine the maximum deceleration (peak value) which could be obtained. The conditions for the simulation terminating were the same as discussed in Section II.

For the tailless version a maximum deceleration of 9 m/s^2 was obtained at a velocity of 5 m/s. When attempting initial velocities greater than this, the robot would topple over.

The model with the actuated tail achieved a peak deceleration of 23 m/s^2 at a maximum velocity of 8 m/s. This did however result in an end tail velocity of ~10 rad/s, which could be detrimental during the experimental testing. Screenshots of the animation produced by the simulation are also shown in Fig. 7.

V. Rapid Acceleration

A. Force Model Identification

The acceleration force was provided by a brushless DC motor (*Traxxas Velineon*) controlled by PWM. As with the braking, we will model this system as a force input disturbance. It is noted that we do have control of this as an input to the system, but to keep uniformity of the control architecture, we will assume it is an input disturbance.

Simple step tests were performed on *Dima* to determine the model parameters. The force equation in the Laplace domain is given by:

$$F_a = k_v \frac{\omega_{mech}}{s + \omega_{mech}} (V_{in} - k_\omega \dot{x}) \qquad (10)$$

where k_v, ω_{mech} and k_ω are model parameters and V_{in} is the voltage input produced by PWM.

Data from a 40% throttle step was used and in a similar method, Matlab's 'lsqnonlin' was employed to fit the parameter values. A comparison between the fit and the experimental data is depicted in Fig. 8.

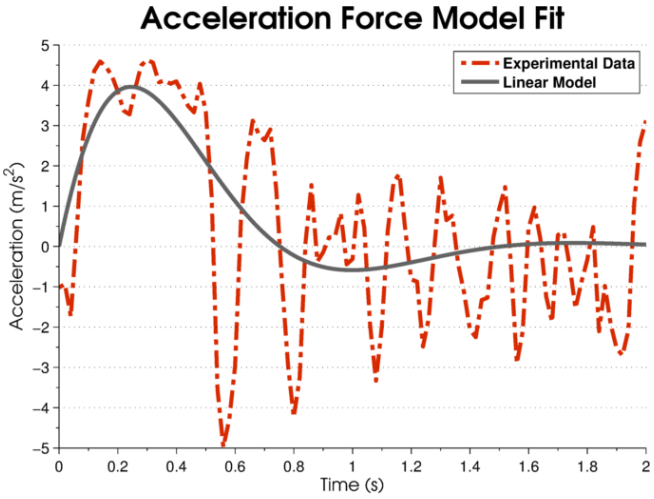

Fig. 8. Linear model fit for the acceleration produced by the brushless DC motor. The data was taken from a 40% throttle step. The oscillations are attributed to the uneven grass where the test occurred.

B. Tail Controller Design

If we consider the acceleration force to be a disturbance, then the same controller architecture can be employed for the acceleration manoeuvres as described in Section IV.

C. Numerical validation

The models were then simulated by stepping the throttle to various values. The performance metric used was the peak acceleration experienced.

The tail-less model obtained a maximum acceleration of 4 m/s^2 at a throttle input of 40%. Any greater steps caused it to pitch over.

The model with an actuated tail obtained an acceleration of 10.8 m/s^2 at throttle input of 90%. However, even with the tail damper discussed, the tail still had an end velocity of 8 rad/s which could be detrimental during experimentation.

VI. Experiments

The tail controller algorithms were then field tested on the robot performing the braking and acceleration manoeuvres. The performance metric for both was the peak accelerations experienced.

Fig. 9. A rapid acceleration test (90% throttle step) with the tail controller is depicted.

The test procedure for braking was as follows:

- The robot would drive straight until attaining the predefined initial velocity
- Then, simultaneously the arrestor system would engage and the robot's motor would stop
- The initial velocity was increased till toppling occurred

For the rapid acceleration tests, the procedure was:

- The throttle would be stepped to a constant value
- Once the tail had reached the end stop, the throttle would be set to zero and the test ended.

A. Results

The results for the rapid deceleration are depicted in Fig. 10. The maximum deceleration for the tailless model was 9.9±0.81 m/s^2 at an initial velocity of 4.5 m/s. The maximum deceleration for the model with the tail was 15.2±0.89 m/s^2 at a velocity of 6.5 m/s.

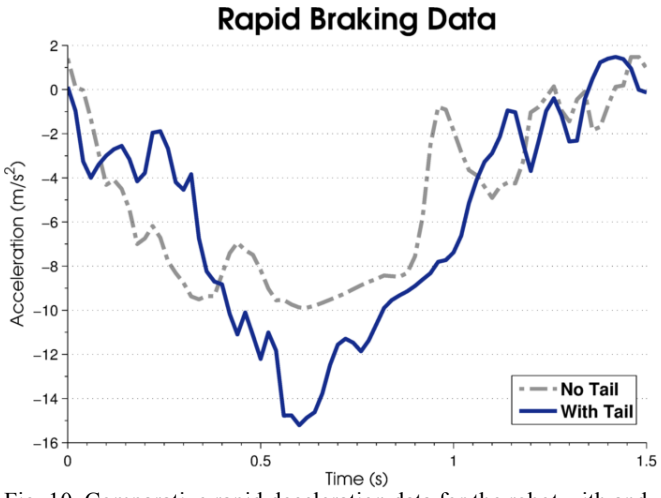

Fig. 10. Comparative rapid deceleration data for the robot with and without the tail.

The results for the rapid acceleration are depicted in Fig. 9 and Fig. 11. The maximum acceleration for the tailless robot was 4.1±0.231 m/s^2.The maximum acceleration for the robot with the tail was 6.1±0.198 m/s^2. The reader is also encouraged to view the attached video comparison (see supplementary material).

VII. Discussion and Conclusion

The tailed robot produced ~50% more acceleration in both test scenarios than the tailless version. But these were still less than those predicted by the simulations.

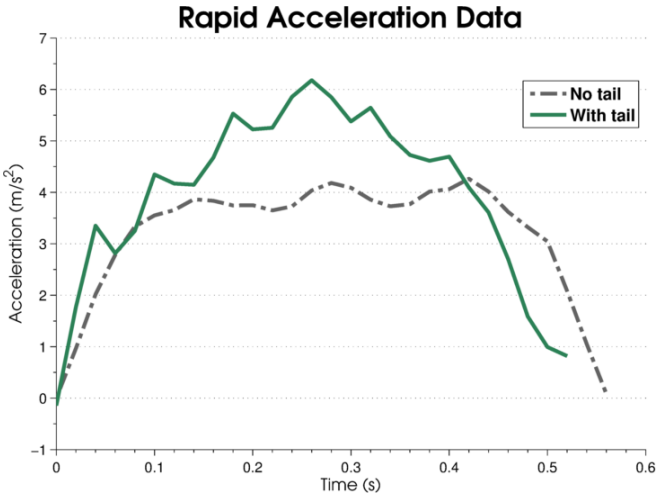

Fig. 11. Comparative experimental data for the acceleration manoeuvre for the tailed and the tailless robot.

For the acceleration tests, this is attributed to the robot's motor controller current limiter as the step tests from 70 to 100% throttle all produced the same accelerations.

However, the chief reason for the difference in both manoeuvres is the tail's end velocity. When attempting more aggressive manoeuvres (braking or accelerating), the tail often struck the end stops with enough velocity to induce a flipping motion. This collision was not accounted for in simulation.

Nevertheless, this study has provided valuable insights for future research. What is evident is that for the cheetah (or a future robot) to optimally use a tail for these tasks, it would need to coordinate the force and the tail trajectories. This would ensure that the tail actuation limits are adhered to, while simultaneously maximising acceleration. Additionally, the cheetah's tail is compliant which means it will absorb any impacts with the body or ground during manoeuvres.

Based on these conclusions possible future robotic implementations should investigate the use of a MIMO optimal controller for manoeuvring using a tail [27] or the design of a compliant (semi-rigid) tail.

Acknowledgment

The authors would like to gratefully acknowledge Callen Fisher and Javaad Patel for their support during testing and the Cheetah Outreach centre. Also, Prof. Ed Boje for advice and contributions to the controller design.

REFERENCES

[1] A. Wilson, J. Lowe, K. Roskilly, P. Hudson, K. Golabek and K. McNutt, "Locomotion dynamics of hunting in wild cheetahs," *Nature,* vol. 498, pp. 185-189, 2013.

[2] P. W. Webb, "Maneuverability - General Issues," *IEEE Journal of Oceanic Engineering,* vol. 29, no. 3, pp. 547-555, 2004.

[3] D. Jindrich and M. Qiao, "Maneuvers during legged locomotion," *Chaos,* vol. 19, 2009.

[4] R. M. Alexander, Principles of Animal Locomotion, Princeton University Press, 2006.

[5] S. Williams, H. T, U. J.R, Wilson and A.M, "Pitch then power: Limitations to acceleration in quadrupeds," *Biology Letters,* vol. 5, pp. 610-613, 2009.

[6] A. Jusufi, D. Kawano, T. Libby and R. Full, "Righting and Turning in mid-air using appendage inertia: Reptile tails, analytical models and bio-inspired robots," *Bioinspiration & Biomimetics,* vol. 5, pp. 1-12, 2010.

[7] C. Walker, V. C and L. Ritz, "Balance in the cat: role of the tail and effects of sacrocaudal transection," *Behavioural Brain Research,* vol. 91, no. 1, pp. 41-47, 1998.

[8] E. Chang-Siu, T. Libby, M. Tomizuka and F. R.J, "A Lizard-Inspired Active Tail Enables Rapid Maneuvers and Dynamic Stabilization in a Terrestrial Robot," in *IEEE/RSJ International Conference on Intelligent Robots and Systems*, San Francisco, California, 2011.

[9] A. Johnson, T. Libby and E. Chang-Siu, "Tail Assisted Dynamic Self Righting," in *Proceedings of the Fifteenth International Conference on Climbing and Walking Robots and the Support Technologies for Mobile Machines*, Baltimore, MD, USA, 2012.

[10] E. Chang-Siu, T. Libby, M. Brown, R. Full and M. Tomizuka, "A nonlinear feedback controller for aerial self-righting by a tailed robot," in *International Conference on Robotics and Automation (ICRA)*, Karlsruhe, 2013.

[11] R. Briggs, J. Lee, M. Haberland and S. Kim, "Tails in Biomimetic Design: Analysis, Simulation and Experiment," in *IEEE/RSJ International Conference on Intelligent Robots and Systems*, Vilamoura, Algarve, Portugal, 2012.

[12] N. Kohut, D. Haldane, D. Zarrouk and R. Fearing, "Effect of Inertial Tail on Yaw Rate of 45 gram Legged Robot," in *Proceedings of the Fifteenth International Conference on Climbing and Walking Robots and the Support Technlogies for Mobile Machines*, Baltimore, MD, USA, 2012.

[13] N. Kohut, A. Pullin, D. Haldane, D. Zarrouk and R. Fearing, "Precise Dynamic Turning of a 10 cm Legged Robot on a Low Friction," in *International Conference on Robotics and Automation (ICRA)*, Karlsruhe, 2013.

[14] A. Patel and M. Braae, "Rapid Turning at High-Speed: Inspirations from the Cheetah's Tail," in *IEEE/RSJ International Conference on Intelligent Robots and Systems (IROS)*, Tokyo, 2013.

[15] A. Patel and M. Braae, "An Actuated Tail Increases Rapid Acceleration Manoeuvres in Quadruped Robots," in *International Joint Conferences on Computer, Information, Systems Sciences and Engineering*, 2012.

[16] R. Full and D. Koditschek, "Templates and Anchors: Neuromechanical hypotheses of legged locomotion on land," *Journal of Experimental Biology,* vol. 202, no. 23, pp. 3325-3332, 1999.

[17] P. Holmes, R. Full, D. Koditschek and J. Guckenheimer, "The dynamics of legged locomotion: Models, analysis and challenges," *SIAM Rev.,* vol. 48, no. 2, pp. 206-304, 2006.

[18] J. Lee, S. Sponberg, O. Loh, G. Lamperski, R. Full and N. Cowan, "Templates and Anchors for Antenna-Based Wall Following in Cockroaches and Robots," *IEEE Transactions on Robotics,* vol. 24, no. 1, pp. 130-143, 2008.

[19] S. Williams, J. Usherwood, K. Jespers, A. Channon and A. Wilson, "Exploring the mechanical basis for acceleration: Pelvic limb locomotor function during accelerations in racing greyhounds (Canis familiaris)," *The Journal of Experimental Biology,* vol. 212, pp. 550-565, 2009.

[20] D. Greenwood, Advanced Dynamics, Cambridge: Cambridge University Press, 2003.

[21] R. Murray, Z. Li and S. Sastry, A Mathematical Introduction to Robotic Manipulation, CRC Press, 1994.

[22] P. Hudson, S. Corr and A. Wilson, "High speed galloping in the cheetah (Acinonyx jubatus) and the racing greyhound (Canis familiaris): spatio-temporal and kinetic characteristics.," *Journal of Experimental Biology,* vol. 215, no. 14, pp. 2425-2434, 2012.

[23] L. Marker and A. Dickman, "Morphology, Physical Condition and Growth of the Cheetah (Acinonyx Jubatus)," *Journal of Mamalogy,* vol. 84, no. 3, pp. 840-850, 2003.

[24] F. Mainardi and G. Spada, "Creep, Relaxation and Viscosity Properties for Basic Fractional Models in Rheology," *The European Physical Journal, Special Topics,* vol. 193, pp. 133-160, 2011.

[25] R. Tedrake, "Fully Actuated vs. Underactuated Systems (Course Notes)," MIT OpenCourseWare, 2009.

[26] A. Shkolnik and R. Tedrake, "High-Dimensional Underactuated Motion Planning via Task Space Control," in *IEEE International Conference on Intelligent Robots and Systems*, 2008.

[27] D. Kirk, Optimal Control Theory: An Introduction, Mineola, New York: Dover Publications, 2004.